

Growth and characterization of single crystal rocksalt LaAs using LuAs barrier layers

E. M. Krivoy, S. Rahimi, H. P. Nair, R. Salas, S. J. Maddox et al.

Citation: *Appl. Phys. Lett.* **101**, 221908 (2012); doi: 10.1063/1.4766945

View online: <http://dx.doi.org/10.1063/1.4766945>

View Table of Contents: <http://apl.aip.org/resource/1/APPLAB/v101/i22>

Published by the [American Institute of Physics](http://www.aip.org).

Related Articles

Investigation of the recombination mechanism of excess carriers in undoped BaSi₂ films on silicon
J. Appl. Phys. **112**, 083108 (2012)

Light-management in ultra-thin polythiophene films using plasmonic monopole nanoantennas
Appl. Phys. Lett. **101**, 151106 (2012)

Effective light management of three-dimensionally patterned transparent conductive oxide layers
Appl. Phys. Lett. **101**, 143904 (2012)

Anomalous Hall effects in Co₂FeSi Heusler compound films and Co₂FeSi-Al₂O₃ granular films
J. Appl. Phys. **111**, 083919 (2012)

Computational study of energy filtering effects in one-dimensional composite nano-structures
J. Appl. Phys. **111**, 024508 (2012)

Additional information on *Appl. Phys. Lett.*

Journal Homepage: <http://apl.aip.org/>

Journal Information: http://apl.aip.org/about/about_the_journal

Top downloads: http://apl.aip.org/features/most_downloaded

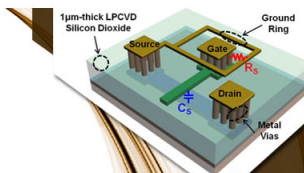
Information for Authors: <http://apl.aip.org/authors>

ADVERTISEMENT



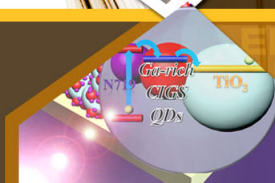
**EXPLORE WHAT'S
NEW IN APL**

SUBMIT YOUR PAPER NOW!



SURFACES AND INTERFACES

Focusing on physical, chemical, biological, structural, optical, magnetic and electrical properties of surfaces and interfaces, and more...



ENERGY CONVERSION AND STORAGE

Focusing on all aspects of static and dynamic energy conversion, energy storage, photovoltaics, solar fuels, batteries, capacitors, thermoelectrics, and more...

Growth and characterization of single crystal rocksalt LaAs using LuAs barrier layers

E. M. Krivoy,^{1,a)} S. Rahimi,¹ H. P. Nair,¹ R. Salas,¹ S. J. Maddox,¹ D. J. Ironside,¹ Y. Jiang,¹ V. D. Dasika,¹ D. A. Ferrer,¹ G. Kelp,² G. Shvets,² D. Akinwande,¹ and S. R. Bank¹

¹Microelectronics Research Center, The University of Texas at Austin, Austin, Texas 78712, USA

²Department of Physics, The University of Texas at Austin, Austin, Texas 78712, USA

(Received 9 August 2012; accepted 26 October 2012; published online 26 November 2012)

We demonstrate the growth of high-quality, single crystal, rocksalt LaAs on III-V substrates; employing thin well-behaved LuAs barrier layers at the III-V/LaAs interfaces to suppress nucleation of other LaAs phases, interfacial reactions between GaAs and LaAs, and polycrystalline LaAs growth. This method enables growth of single crystal epitaxial rocksalt LaAs with enhanced structural and electrical properties. Temperature-dependent resistivity and optical reflectivity measurements suggest that epitaxial LaAs is semimetallic, consistent with bandstructure calculations in literature. LaAs exhibits distinct electrical and optical properties, as compared with previously reported rare-earth arsenide materials, with a room-temperature resistivity of $\sim 459 \mu\Omega\text{-cm}$ and an optical transmission window $>50\%$ between $\sim 3\text{-}5 \mu\text{m}$. © 2012 American Institute of Physics. [<http://dx.doi.org/10.1063/1.4766945>]

The semimetallic properties of the rare-earth monpnictides (RE-V), as well as their ability to be epitaxially embedded as buried films^{1,2} and nanostructures³ within high-quality III-V semiconductors, makes them attractive for a variety of device applications. Examples include high-performance tunnel junctions for multijunction solar cells,⁴ epitaxial transparent Ohmic contacts for photonic devices,⁵ epitaxial low resistance Ohmic contacts for high-frequency electronics,⁶ thermoelectrics,⁷ and plasmonic enhancement in various devices.⁸ In particular, a family of epitaxially compatible semimetals that offer a diversity of optical properties could enable the integration of tailored metallic structures into the core of nanophotonic devices, creating new opportunities for device design and functionality.

The RE-Vs can be integrated epitaxially with conventional zinc-blende III-V materials under typical growth conditions, resulting in high-quality epitaxial interfaces.^{1,3} Promising results from Er-V materials motivate a thorough investigation of the other RE-V materials. However, many of the RE-V monpnictides, including LaAs, have additional stable RE-rich and group-V-rich phases. The La-As material system has three known stable crystalline phases: LaAs, LaAs₂, and La₄As₃,⁹ which may each form under different sets of growth conditions; this greatly increases the difficulty in determining fundamental material properties and inhibits potential device applications. In spite of these challenges, LaAs is particularly attractive for initial investigations as it represents an endpoint of the lanthanide series, potentially providing insight into the range of available materials properties, and has the largest lattice constant of the RE-As materials. The rocksalt phase of LaAs has a lattice constant of 6.1504 \AA , and is closely lattice-matched to the 6.1 \AA family of III-V zincblende semiconductors.¹⁰ More broadly, understanding how the rare-earth species affects the proper-

ties of RE-V materials could elucidate the diversity of accessible parameters achievable in the RE-V material system.

Initial attempts to grow LaAs directly on GaAs and InAs substrates resulted in polycrystalline films with poor surface morphology over a wide range of molecular beam epitaxy (MBE) growth conditions, possibly due to a combination of both nucleation of additional La-As stable phases and interfacial reactions with the III-V materials. Based on these preliminary findings, we developed a technique for the growth of high-quality LaAs utilizing thin LuAs barrier layers at the RE-V/III-V heterointerfaces, and characterized the basic electrical, optical, and structural properties of rocksalt epitaxial single-crystalline LaAs.

Samples were grown by solid-source MBE in an EPI Mod. Gen. II system. Samples without LuAs layers, shown schematically in Fig. 1(a), consisted of (100) semi-insulating GaAs substrates with a (a) 200 nm GaAs buffer, followed by (b) 5-67 nm of LaAs, and a (c) 15-30 nm GaAs cap. The growth parameter space was first investigated to attempt to isolate the growth of rocksalt LaAs. Sweeping substrate temperature from 390 to 500 °C, arsenic overpressure from $15\times$ to $50\times$ over the La beam-equivalent pressure (BEP), and growth rate from 0.05 to 0.1 monolayers/second (ML/s), failed to identify a growth regime for single-crystalline rocksalt LaAs. The reflection high-energy electron diffraction (RHEED) patterns observed *in situ* during growth (Fig. 2(a)) were indicative of polycrystalline films with poor surface morphology, under all growth conditions. Higher-order diffraction patterns, as well as severe chevroning, were observed in the RHEED patterns, suggesting poor quality films. LaAs films grown on nearly lattice-matched (100) n-type InAs substrates showed similarly poor RHEED patterns, indicating that strain relaxation was unlikely the cause of the degraded films. Samples were also analyzed *ex situ* using X-ray diffraction (XRD); Fig. 3 plots ω - 2θ scans exhibiting both the anticipated LaAs peaks, as well as multiple anomalous peaks, consistent with RHEED observations.

^{a)}Author to whom correspondence should be addressed. Electronic mail: erica.krivoy@mail.utexas.edu.

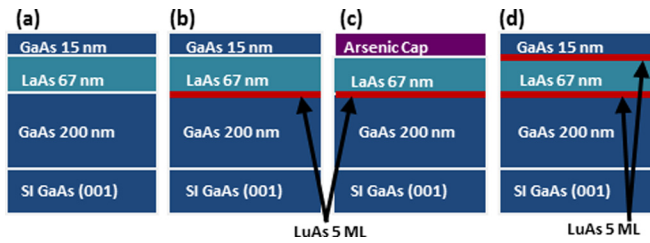


FIG. 1. Layer structures for LaAs growth on (100) GaAs. (a) LaAs layer grown directly between GaAs layers, (b) LaAs grown on a thin LuAs layer, (c) LaAs grown on a thin LuAs layer with arsenic cap, and (d) LaAs grown between thin LuAs layers.

Powder diffraction data¹¹ for the La-As stable phases and various crystalline orientations of rocksalt LaAs failed to definitively clarify the origin of the anomalous peaks, suggesting a mixture of effects during the growth of the LaAs on GaAs.

Unlike LaAs, LuAs forms in a single rocksalt phase.¹⁰ Additionally, like ErAs, LuAs has been shown to grow with high-quality on III-V substrates,^{1,12} and is nearly lattice-matched to GaAs. In order to suppress the formation of non-rocksalt phases on (100) III-V substrates, we inserted a thin coherent LuAs barrier layer, as sketched in Fig. 1(b), between the GaAs buffer and LaAs films. The initial motivation was to use the LuAs thin film as a rocksalt template to seed a single-phase LaAs rocksalt growth. Moreover, LuAs has been observed to be well-behaved on GaAs,¹² it could provide a more stable crystalline template for the nucleation of LaAs. Bright, streaky, 1×1 RHEED patterns were observed Fig. 2(b) for LaAs films grown at 460 °C and 46:1 RE:As BEP ratio on GaAs below the critical thickness; as shown in Fig. 2(c), slightly degraded surface morphology was observed in the RHEED pattern after the LaAs film exceeded the critical thickness. However, no polycrystalline rings were observed in the RHEED patterns of films grown using the LuAs barrier layer. Both 5 and 10 ML of coherent LuAs were investigated as barrier layers, but no discernible difference was observed in the quality of the LaAs growth between the two thicknesses. For LaAs grown on n-type InAs substrates, a 2.5 ML LuAs seed was employed to avoid strain relaxation of the highly lattice-mismatched LuAs on InAs. In the ω - 2θ scans of these samples, no peaks from other La-As phases were detected.

Even with this improvement, the ω - 2θ scan (Fig. 3(b)) still showed one remaining anomalous peak at an angle of $\sim 13.5^\circ$, whose corresponding lattice parameter exceeded that of LaAs. Varying growth parameters did not affect its

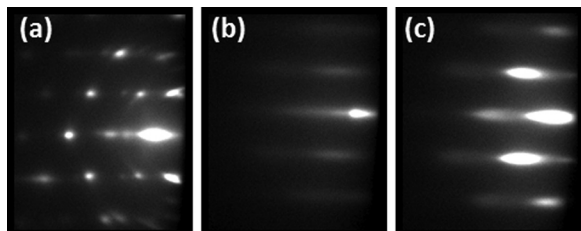


FIG. 2. RHEED patterns of LaAs growth. (a) Polycrystalline RHEED pattern of LaAs on GaAs, (b) LaAs grown on a LuAs layer before reaching critical thickness, and (c) LaAs grown on a LuAs layer after critical thickness.

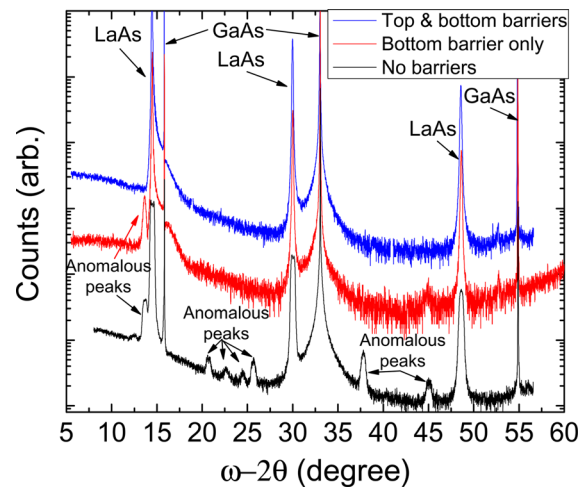


FIG. 3. XRD ω - 2θ scans showing the (002), (004), and (006) reflections. Anomalous peaks are visible in the sample without the LuAs bottom barrier layer, and disappear with the addition of an underlying LuAs barrier. A low-angle anomalous peak was observed in samples grown with the bottom LuAs barrier layer only. This low-angle peak was not observed in the samples grown with top and bottom LuAs barrier layers.

peak intensity or position. Suspecting interfacial reactions between the Ga, La, and As at the potentially unstable top LaAs/GaAs interface, growth was repeated with a thick arsenic cap grown directly on top of the LaAs layer to prevent oxidation of the LaAs film rather than the standard GaAs cap. The XRD ω - 2θ scan of the arsenic-capped sample exhibited no anomalous peaks. Additionally, as shown in Fig. 3, inserting a second thin LuAs layer between the LaAs film and GaAs cap similarly suppressed the anomalous peak at $\sim 13.5^\circ$. Instability of the LaAs/GaAs and LaAs/InAs interfaces may be explained by the comparable enthalpies of formation, given in Table I, between LaAs, LaGa, and LaIn.¹³ In contrast, the enthalpies of formation for LuAs, LuGa, and LuIn may be sufficiently dissimilar to prevent interfacial interactions at heterointerfaces. This is consistent with observations of the well-behaved ErAs/GaAs and ErAs/InAs systems, which, similar to the LuAs/GaAs and LuAs/InAs systems, have dissimilar enthalpies of formation.¹³ Additionally, Schultz *et al.* observed that nucleating nanostructures of ErSb on GaSb substrates form a diffusion barrier, limiting the interaction of Er and the GaSb layer underneath.¹⁴ The LuAs layer may, therefore, limit interfacial reactions between La and Ga. However, it has been observed that as ErSb nanostructures nucleate on GaSb substrates, the Ga atoms are displaced to the surface, where they become available to bond.¹⁴ In the case of LaAs/LuAs/GaAs, there may still be a small concentration of surface Ga atoms interacting with La atoms, regardless of the LuAs barrier layers, possibly resulting in interfacial reactions. Thin RE-V films have been employed as diffusion barriers in metal/semiconductor growth by Schultz *et al.* in the growth of Fe/GaAs,¹⁵ in $\text{Co}_2\text{NiGa}/\text{GaAs}$ by Shih *et al.*,¹⁶ and in CoTiSb by Kawasaki *et al.*¹⁷ Therefore, the poor quality growth of LaAs directly on GaAs may result from both competing phase formation and interfacial reactions at the heterointerfaces due to comparable enthalpies of formation for LaAs and LaGa. The thin LuAs barriers may, therefore, serve a dual purpose: first, as a template for the initial

TABLE I. Enthalpies of formation for various RE-V and RE-III compounds.

	Arsenic (kJ/mol) ¹³	Gallium (kJ/mol) ¹³	Indium (kJ/mol) ¹³	Multiple RE-V phases? ¹³
Lutetium	-75.6	-52.2	-34.7	N
Lanthanum	-73	-68.6	-65	Y

nucleation of rocksalt LaAs, and second, as a barrier to prevent interfacial reactions of Ga, La, and As at the heterointerfaces.¹⁴ Further investigations into the root cause of poor-quality LaAs on III-V growth are underway; however, regardless of the precise effects of the thin LuAs barrier layers, utilizing them enabled the growth of high-quality epitaxial LaAs films.

(224) asymmetrical reciprocal space maps (RSM) of a 67 nm (Fig. 4) and a 500 nm LaAs film (not shown) indicate a nearly fully relaxed film. A similar residual strain of $\sim 1\%$ was observed for both film thicknesses, and may be as result of a difference in thermal expansion coefficients between GaAs and the RE-Vs.¹⁸ Surface morphology is an important consideration for potential device applications. To this end, surface roughness of the different structures was characterized with tapping-mode atomic force microscopy (AFM). A Veeco Dimension ICON atomic force microscope was employed to obtain surface topography images at room-temperature, under ambient atmosphere, with a silicon probe tip. Surface roughness was measured for scan areas of $3 \times 3 \mu\text{m}^2$ for samples grown on GaAs with 15 nm of GaAs cap on top of the RE-V layers to prevent oxidation. The RMS roughness for LaAs films grown with and without bottom LuAs barrier layers was 1.43 ± 0.07 nm and 1.9 ± 0.02 nm, respectively, suggesting that the LuAs barrier layers only modestly improved surface morphology. Samples were prepared for cross-sectional transmission electron microscopy (TEM) using mechanical lapping and argon ion milling. High-resolution TEM images were taken of samples with and without a bottom LuAs barrier layer. When LaAs was grown on a LuAs barrier on GaAs, the resulting film was found to be highly crystalline in nature, as seen in Fig. 5(a). The fast Fourier transform (FFT) analysis of the interface (Fig. 5(b)), which was used as a good approximation to the selected area diffraction (SAD) pattern, suggests a

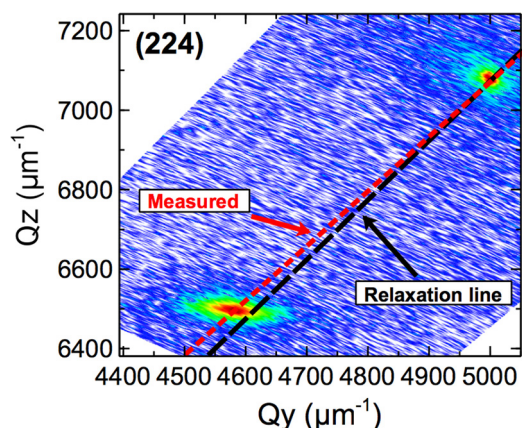


FIG. 4. Asymmetric (224) RSM of 67 nm of LaAs, with top and bottom LuAs barrier layers, showing residual strain in film of $\sim 1\%$.

continuous crystalline sub-lattice of the arsenic anions.¹⁹ In contrast, LaAs grown directly on GaAs resulted in a polycrystalline film (Fig. 5(d)) whose interface exhibited multiple polycrystalline spots (Fig. 5(c)) in the FFT pattern. Further studies will investigate defect density and propagation in LaAs grown on III-V.²⁰

Temperature-dependent resistivity measurements, shown in Fig. 6, of a 500 nm film of LaAs grown between 10 ML LuAs top and bottom barrier layers exhibited a room-temperature resistivity of $\sim 593 \mu\Omega\text{-cm}$ and a variation in resistivity of $\sim 2\times$ over the 77-300 K range. The resistivity of the film increased with increasing temperature, consistent with metallic behavior.²¹ The effect of parallel resistances in the LaAs with LuAs barrier layers was accounted for using a 10 ML LuAs sample. We observed a $\sim 20\%$ reduction in the room-temperature resistivity of a 67 nm film of LaAs grown without and with the LuAs barrier layers, from $566 \mu\Omega\text{-cm}$ without LuAs barriers to $459 \mu\Omega\text{-cm}$ with barriers, which, along with the observed improvement in the XRD ω -2 θ scans, strongly suggests that LuAs interfacial layers significantly enhance the quality of the LaAs. Preliminary results from temperature-dependent resistivity measurements of LaAs grown with and without barriers suggest that the improvement may be even more pronounced. LaAs films grown without the LuAs barrier layers exhibit a larger difference in resistivity between room-temperature and 77 K measurements than films grown with LuAs barriers. At low temperatures, the effect of thermally activated phonon-electron scattering is reduced and, therefore, the effect of carrier scattering due to poor film quality is more pronounced. Because the film with LuAs barriers have less dependence on temperature than those without, this suggests that the LuAs barrier layers improved the quality of the LaAs film.²² The disparity between the resistivity values of the 67 nm and 500 nm LaAs films may be attributable to a decrease in film quality due to an increase in defect density with increasing thickness. Indeed, *in situ* observations of RHEED during growth indicated decreased long-range order with increasing thickness, suggesting a roughening in the growing film. LaAs has a larger room-temperature resistivity than those reported for LuAs^{1,12} and ErAs,¹ potentially due to a number of effects stemming from differences in band structure and carrier concentrations.^{23,24}

Optical characterization was conducted on a $0.5 \mu\text{m}$ LaAs film using Fourier transform infrared spectroscopy (FTIR), shown in Fig. 7. The peak transmission window of LaAs, with transmittance above 20% in the wavelength

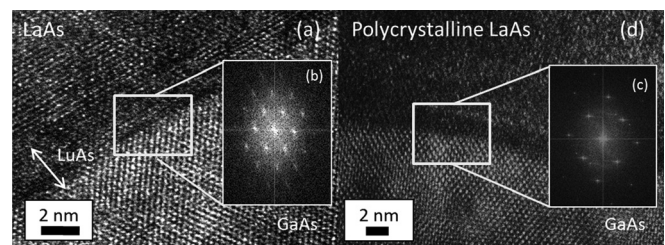


FIG. 5. HRTEM images of LaAs grown with and without LuAs barrier layers on GaAs. (a) LaAs layer grown on a thin LuAs layer, (b) FFT analysis approximating SAD pattern of LaAs/GaAs interface, (c) FFT pattern of LaAs/LuAs/GaAs interface, and (d) LaAs grown directly on GaAs.

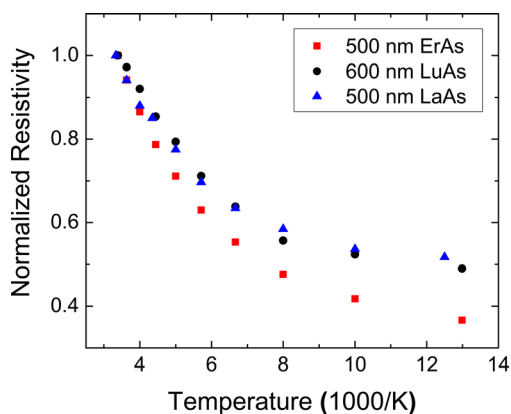


FIG. 6. Temperature-dependent resistivity of LuAs, ErAs, and LaAs films normalized to their respective room-temperature resistivities. LaAs resistivity varied by $\sim 2\times$ over the range of 77–300 K, similarly to what is observed for LuAs and ErAs.

range of $\sim 3\text{--}8\ \mu\text{m}$, is noticeably different than those of LuAs¹² and ErAs,⁵ being both much broader and occurring at longer wavelengths. This demonstrates that it is possible to manipulate the optical properties of RE-V materials through the choice of the rare-earth element. Additionally, the reflectivity measurements, shown in Fig. 7, suggest that LaAs possesses a Drude edge below $\sim 0.2\ \text{eV}$, in agreement with measurements by Kimura *et al.*²⁵ The apparent Drude edge, combined with the metal-like temperature-dependent resistivity, and theoretical band structure calculations,²³ suggests that LaAs is semimetallic.

The growth of high-quality LaAs on GaAs substrates was demonstrated using LuAs barrier layers. Films were characterized optically, electrically, and structurally and showed distinct properties from previously studied epitaxial RE-As materials. Further investigation is needed to understand the issues surrounding the growth of high-quality single-phase rocksalt LaAs on III-V substrates and to determine the root causes of the beneficial effects of LuAs barrier layers. In particular, high-resolution scanning transmission electron microscopy (HRTEM) and energy dispersive X-ray spectroscopy could be used to study the interfaces of GaAs/

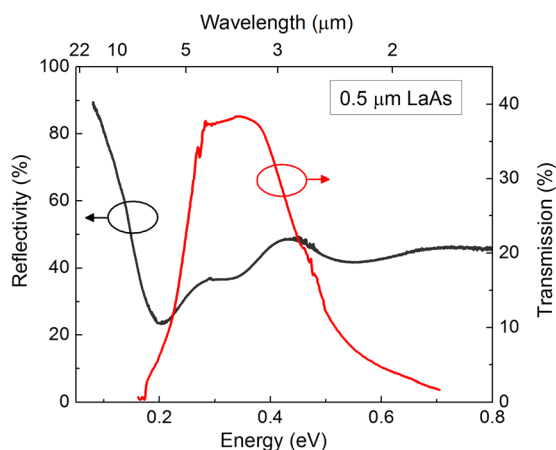


FIG. 7. Reflectivity and transmission spectra of $0.5\ \mu\text{m}$ of LaAs. The Drude edge appears at photon energies below $\sim 0.2\ \text{eV}$. Transmission spectrum has peak wavelengths of $\sim 3.5\text{--}6\ \mu\text{m}$ above 35% transmittance.

LuAs/LaAs and GaAs/LaAs in more depth. In conclusion, thin LuAs barrier layers enabled the growth of single-crystalline epitaxial rocksalt LaAs with enhanced structural quality and electrical properties. This approach has the potential to be applied to other RE-V compounds that exhibit unstable interfaces when grown on III-V materials and/or multiple stable RE-V phases.

This work was supported by the ARO through the PECASE Program (W911NF-09-1-0434) monitored by Dr. Dwight Woolard, by the ARO through the YIP Program (W911 NF-11-1-0455), and by the AFOSR through the YIP (FA9550-10-1-0182) monitored by Dr. Kitt Reinhardt.

- ¹C. J. Palmström, K. C. Garrison, S. Mounier, T. Sands, C. Schwartz, N. Tabatabaie, S. Allen, H. Gilchrist, and P. Miceli, *J. Vac. Sci. Technol. B* **7**, 747–752 (1989).
- ²A. M. Crook, H. P. Nair, D. A. Ferrer, and S. R. Bank, *Appl. Phys. Lett.* **99**, 072120 (2011).
- ³C. Kadow, S. B. Fleischer, J. P. Ibbetson, J. E. Bowers, A. C. Gossard, J. W. Dong, and C. J. Palmström, *Appl. Phys. Lett.* **75**, 3548 (1999).
- ⁴J. M. O. Zide, A. Kleiman-Shwarscstein, N. C. Strandwitz, J. D. Zimmerman, T. Steenblock-Smith, A. C. Gossard, A. Forman, A. Ivanovskaya, and G. D. Stucky, *Appl. Phys. Lett.* **88**, 162103 (2006).
- ⁵M. P. Hanson, A. C. Gossard, and E. R. Brown, *Appl. Phys. Lett.* **89**, 111908 (2006).
- ⁶U. Singiseti, M. A. Wistey, J. D. Zimmerman, B. J. Thibeault, M. J. W. Rodwell, A. C. Gossard, and S. R. Bank, *Appl. Phys. Lett.* **93**, 183502 (2008).
- ⁷W. Kim, J. Zide, A. Gossard, D. Klenov, S. Stemmer, A. Shakouri, and A. Majumdar, *Phys. Rev. Lett.* **96**, 045901 (2006).
- ⁸M. P. Hanson, A. C. Gossard, and E. R. Brown, *J. Appl. Phys.* **102**, 043112 (2007).
- ⁹K. Gschneidner and F. Calderwood, *J. Phase Equilib.* **7**, 274–276 (1986).
- ¹⁰T. Sands, C. J. Palmström, J. P. Harbison, V. G. Keramidas, N. Tabatabaie, T. L. Cheeks, R. Ramesh, and Y. Silberberg, *Mater. Sci. Rep.* **5**, 99 (1990).
- ¹¹S. Ono, J. G. Despault, L. D. Calvert, and J. B. Taylor, *J. Less Common Metals* **22**, 51 (1970).
- ¹²E. M. Krivoy, H. P. Nair, A. M. Crook, S. Rahimi, S. J. Maddox, R. Salas, D. A. Ferrer, V. D. Dasika, D. Akinwande, and S. R. Bank, *Appl. Phys. Lett.* **101**, 141910 (2012).
- ¹³C. Colinet, *J. Alloys Compd.* **225**, 409–422 (1995).
- ¹⁴B. D. Schultz, S. G. Choi, and C. J. Palmström, *Appl. Phys. Lett.* **88**, 243117 (2006).
- ¹⁵B. D. Schultz, *In-Situ Surface, Chemical, Electrical Characterization of the Interfaces between Ferromagnetic Metals and Compound Semiconductors Grown by Molecular Beam Epitaxy* (The University of Minnesota, 2005).
- ¹⁶T. C. Shih, J. Q. Xie, J. W. Dong, X. Y. Dong, S. Srivastava, C. Adelman, S. McKernan, R. D. James, and C. J. Palmström, *Ferroelectrics* **342**, 35 (2006).
- ¹⁷J. K. Kawasaki, L. M. Johansson, M. Hjort, R. Timm, B. D. Schultz, and C. J. Palmström, in 29th North American Molecular Beam Epitaxy Conference, Stone Mountain Georgia, October 2012.
- ¹⁸L. J. Brillson, *Contacts to Semiconductors: Fundamentals and Technology*, 1st ed. (Noyes, New Jersey, 1994).
- ¹⁹J. G. Zhu, C. B. Carter, C. J. Palmström, and S. Mounier, *Appl. Phys. Lett.* **56**, 1323 (1990).
- ²⁰P. F. Miceli, C. J. Palmström, and K. W. Moyers, *Appl. Phys. Lett.* **58**, 1602 (1991).
- ²¹S. J. Allen, Jr., F. DeRosa, C. J. Palmström, and A. Zrenner, *Phys. Rev. B* **43**, 9599 (1991).
- ²²J. Singleton, *Band Theory and Electronic Properties of Solids* (Oxford University Press, 2001).
- ²³E. Deligöz, K. Çolakoglu, Y. Ö. Çiftçi, and H. Özişik, *J. Phys.: Condens. Matter* **19**, 436204 (2007).
- ²⁴A. G. Petukhov, W. R. L. Lambrecht, and B. Segall, *Phys. Rev. B* **53**, 4324 (1996).
- ²⁵S. Kimura, F. Arai, Y. Haga, T. Suzuki, and M. Ikezawa, *Phys. B: Condens. Matter* **206**, 780–782 (1995).